Acta Crystallographica Section D
Biological Crystallography
ISSN 0907-4449

High-resolution structure of human phosphoserine phosphatase in open conformation

Yves Peeraer,[a] Anja Rabijns,[a]* Christel Verboven,[a] Jean-François Collet,[b] Emile Van Schaftingen[b] and Camiel De Ranter[a]

[a]Laboratory for Analytical Chemistry and Medicinal Physicochemistry, Faculty of Pharmaceutical Sciences, K.U. Leuven, E. Van Evenstraat 4, B-3000 Leuven, Belgium, and [b]Laboratory of Physiological Chemistry, Christian de Duve Institute of Cellular Pathology, Université Catholique de Louvain, B-1200 Brussels, Belgium

Correspondence e-mail: anja.rabijns@pharm.kuleuven.ac.be

Received 11 November 2002
Accepted 6 March 2003

PDB Reference: phosphoserine phosphatase, 1nnl, r1nnlsf.

The crystal structure of human phosphoserine phosphatase (HPSP) in the open conformation has been determined at a resolution of 1.53 Å. The crystals are orthorhombic, belonging to space group $C222_1$, with unit-cell parameters a = 49.03, b = 130.25, c = 157.29 Å. The asymmetric unit contains two molecules. Phase information was derived from a multi-wavelength anomalous dispersion (MAD) experiment conducted at three wavelengths using a selenomethionine-derivative crystal of HPSP. The structure was refined using *CNS* to a final crystallographic R value of 21.6% ($R_{\rm free}$ = 23.4%). HPSP is a dimeric enzyme responsible for the third and final step of the L-serine biosynthesis pathway. It catalyses the Mg^{2+}-dependent hydrolysis of L-phosphoserine. Recently, the structure of HPSP in complex with an inhibitor bound to the active site has been reported to be the open conformation of the enzyme. Here, the structure of HPSP is reported in the absence of substrate in the active site. Evidence is presented that HPSP in an uncomplexed form is in an even more open conformation than in the inhibitor complex. In this state, the enzyme is partially unfolded to allow the substrate to enter the active site. Binding of the substrate causes HPSP to shift to the closed conformation by stabilizing the partially unfolded region. In the present structure a Ca^{2+} ion is bound to the active site and an explanation is given why HPSP is not active when in the active site Mg^{2+} is replaced by a Ca^{2+} ion.

1. Introduction

L-Serine is a non-essential amino acid synthesized *de novo* from 3-phosphoglycerate, a glycolytic intermediate. L-Serine is not only a building block for protein synthesis, but is also a precursor of a number of compounds, including phospholipids (phosphatidylserine and sphingomyelin) and glycolipids. The rate-limiting step in the biosynthesis of L-serine in mammalian cells is the hydrolysis of L-phosphoserine by phosphoserine phosphatase (PSP). PSP is a dimeric enzyme which requires Mg^{2+} for maximal activity.

The present paper discusses the three-dimensional structure of human phosphoserine phosphatase (HPSP). One monomer of HPSP contains 225 residues and has a relative molecular mass of 25 kDa (Collet *et al.*, 1997). L-Serine is a negative-feedback inhibitor which regulates the metabolic activity of HPSP. During the course of the reaction, a phosphoaspartate adduct is formed near the active site. The phosphorylated aspartate is the first residue of a conserved D*X*D*X*(T/V) motif. Notably, this motif has been found in many other phosphatases or phosphomutases (Collet *et al.*, 1998).

HPSP is probably one of the best characterized members of a superfamily of enzymes comprising P-type ATPases, haloacid dehalogenase and phosphotransferases (Aravind *et*

al., 1998; Collet *et al.*, 1998; Ridder & Dijkstra, 1999). Sequence comparison shows that the members of this haloacid dehalogenase (HAD) superfamily share three statistically significant and highly conserved sequence motifs. The residues belonging to these motifs are located in the active site. The first of these motifs contains an absolutely conserved aspartate that forms the covalent intermediate. The second motif contains a conserved serine or threonine residue and the third motif contains a strictly conserved lysine residue followed, at some distance, by less conserved residues and a strictly conserved aspartate. Mutation of these conserved residues shows that all three motifs play an important role in the catalytic process (MacLennan *et al.*, 1992; Lingrel & Kuntzweiler, 1994; Collet *et al.*, 1999). Several cases of congenital defects in the biosynthesis of L-serine have been reported. One of these arises from HPSP deficiency (Jaeken *et al.*, 1996).

There is also evidence that HPSP may play an important role in the regulation of the D-serine level in the brain. Indeed, L-serine is converted into D-serine through direct racemization by a racemase localized in the brain (Wolosker *et al.*, 1999). Furthermore, D-serine distribution in the brain correlates with the distribution of *N*-methyl-D-aspartate (NMDA) receptors (Dunlop & Neidle, 1997). The NMDA receptor is one of the four varieties of glutamate receptors, a major neurotransmitter receptor family in the nervous system of mammals. The NMDA receptor is involved in functions such as learning and memory. Activation of NMDA receptor channels requires both glutamate and stimulation of a 'glycine site' (Schell *et al.*, 1997). D-Serine is an endogenous ligand for this site and is up to three times more potent than glycine itself (Paudice *et al.*, 1998).

Wang and coworkers were the first to report structural studies on PSP, *i.e.* PSP from *Methanococcus jannaschii* (MJ; Wang *et al.*, 2001; Cho *et al.*, 2001). HPSP shares 31% sequence identity and 52% similarity with MJ PSP and an alignment of the sequences is shown in Fig. 1. Further studies on MJ PSP suggest that during catalysis there is a conformational rearrangement of the active site (Wang *et al.*, 2002). MJ PSP is partially unfolded in the open state. Binding of the substrate L-phosphoserine causes the refolding of this unfolded region and this mechanism provides specificity for the substrate. The subsequent Mg^{2+}-dependent hydrolysis of L-phosphoserine to L-serine is catalysed by MJ PSP in the closed conformation.

Recently, the structure of HPSP in complex with ligands has also been reported (Kim *et al.*, 2002). In the complex with the competitive inhibitor 2-amino-3-phosphonopropionic acid (AP3), determined at a resolution of 2.5 Å, two molecules, MolA and MolB, are present in the asymmetric unit. MolA is in the closed conformation, whereas MolB is described as being in an open conformation.

The present structure determined at a resolution of 1.53 Å provides for the first time a detailed model of the active site in a completely open conformation and the water molecules bound to it. The importance of the present model is that it may provide an additional framework for inhibitor design.

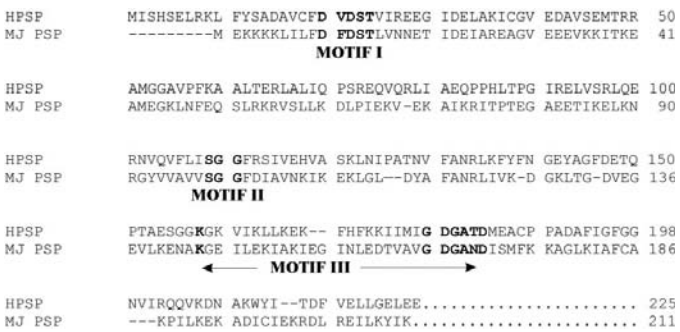

Figure 1
Structure-based sequence alignment of HPSP and MJ PSP. The '–' represent gaps. The three highly conserved sequence motifs of the HAD superfamily are shown in bold.

2. Materials and methods

2.1. Crystallization

The expression, purification and crystallization of HPSP was performed using previously described methods (Peeraer *et al.*, 2002). The protein was dissolved in a buffer at pH 9 containing 25 m*M* glycine and 1 m*M* dithiothreitol. Well diffracting crystals were obtained by the vapour-diffusion method in hanging drops. The crystallization condition consisted of 0.7 *M* $CaCl_2$, 0.1 *M* cacodylate buffer pH 6.3 and 20% polyethylene glycol 1500. The drop contained 1.5 µl of 6.0 mg ml^{-1} protein solution and 1.5 µl of the crystallization condition solution. The well contained 700 µl of the same crystallization condition solution.

2.2. Data collection

A native data set was collected at 100 K using synchrotron radiation (beamline BW7B of the DESY synchrotron, Hamburg) after soaking the PSP crystals for 24 h in a solution of the mother liquor containing 22% polyethylene glycol 400. Crystals grew in space group $C222_1$, diffract to a resolution of 1.53 Å and have unit-cell parameters $a = 49.03$, $b = 130.25$, $c = 157.29$ Å. The data were integrated and merged with *DENZO* and *SCALEPACK* (Otwinowski & Minor, 1997). The final data set is 99.8% complete and is characterized by an $R_{\rm sym}$ of 3.5%. According to Matthews coefficient calculations (Matthews, 1974) the asymmetric unit consists of two molecules, with a corresponding $V_{\rm M}$ of 2.53 $Å^3$ Da^{-1} and a solvent content of 51%.

A selenomethionine derivative of HPSP for phase determination was prepared and crystallized under identical conditions as the native HPSP. The crystals belong to the same space group and have identical unit-cell parameters as the native crystals. A MAD data set was collected to a resolution of 2.50 Å (beamline BW7A of the DESY synchrotron, Hamburg) at three wavelengths from a single selenomethionine-derivative crystal maintained at 100 K. The data-collection statistics for the MAD data set are summarized in Table 1.

Table 1
Data-collection statistics for the MAD data set of the selenomethionine derivative of HPSP at three wavelengths.

Values in parentheses refer to the highest resolution shell (2.54–2.50 Å).

Data set	Wavelength (Å)	Multiplicity	Completeness (%)	Completeness ($I > 2\sigma$) (%)	R_{sym} (%)	$\langle I/\sigma(I)\rangle$
Peak	0.9759	6.3	99.9 (100.0)	95.6 (86.5)	4.9 (15.0)	23.18 (11.26)
Inflection	0.9764	5.0	99.9 (100.0)	93.9 (82.7)	3.5 (17.2)	30.09 (7.25)
Remote	0.9464	4.6	99.8 (99.8)	94.3 (85.8)	4.5 (14.4)	19.55 (9.20)

Table 2
Refinement statistics for the HPSP structure at 1.53 Å resolution.

Final R_{work} (%)	21.6
Final R_{free} (%)	23.4
Refined model	
Protein atoms	3203
Water molecules	390
Ca^{2+} atoms	3
Cl^- atoms	6
Average atomic *B* factors (Å^2)	
Main chain	24.6
Side chain	27.3
Water molecules	34.4
Ca^{2+} atoms	17.6
Cl^- atoms	23.8
R.m.s. deviation of the model	
Bond lengths (Å)	0.005
Bond angles (°)	1.144
B, bonded main chain (Å^2)	1.194
B, bonded side chain (Å^2)	2.077

3. Determination and refinement of the structure

The anomalous difference Patterson map of the peak-wavelength data was calculated using *PHASES* (Furey & Swaminathan, 1997). This Patterson map was used to determine the heavy-atom positions. Visual inspection of the Harker sections revealed a pattern of peaks that could be explained by the presence of four major sites in the asymmetric unit.

Refinement of the heavy-atom positions and phase calculation were performed with the program *SHARP* (de La Fortelle & Bricogne, 1997). The phasing power for the anomalous signal at the peak wavelength was 3.37 for the acentric reflections and the overall figure of merit was 0.64 for the acentric data. *SOLOMON* (Abrahams & Leslie, 1996) solvent flattening of the *SHARP* map gave an electron-density map with clear density for two copies of HPSP in the asymmetric unit. An almost complete model (188/225 residues for each molecule of the asymmetric unit) was built into this experimental map and docked into the known sequence using the *warpNtrace* mode of *ARP*/*wARP* (Perrakis *et al.*, 1999).

The model was subjected to several rounds of crystallographic refinement against the 1.53 Å resolution native data using the program *CNS* (Brünger *et al.*, 1998). All data were included in the refinement. A random test set of 5% of the unique reflections was set apart to calculate R_{free} values as an independent validation of the refinement process. The *R* value of the starting model as generated by *ARP*/*wARP* was 32.8%. Simulated annealing was used for refinement of the model and bulk-solvent correction was used. The two molecules in the asymmetric unit were refined independently; at no time were NCS restraints used between the two molecules in the asymmetric unit. At all stages, σ_A-weighted omit $2|F_{obs}| - |F_{calc}|$ and $|F_{obs}| - |F_{calc}|$ Fourier electron-density maps were calculated and inspected with the program *O* (Jones *et al.*, 1991) to check the agreement of the model with the data. Whenever necessary the model was manually adjusted in *O*. During refinement, solvent molecules were progressively added when they met the following requirements: (i) a minimum 3σ peak had to be present in the $|F_{obs}| - |F_{calc}|$ difference map, (ii) a peak had to be clearly visible in the $2|F_{obs}| - |F_{calc}|$ map, (iii) the *B* value for the water molecules did not exceed 55 Å^2 during refinement and (iv) the water molecules had to be stabilized by hydrogen bonding. Assessment of the quality of the model was performed with *PROCHECK* (Laskowski *et al.*, 1993) and unusual stereochemical features were adjusted if necessary.

Molecular graphics were generated with *MOLSCRIPT* (Kraulis, 1991) and *Raster3D* (Merritt & Bacon, 1997).

4. Results and discussion

4.1. Quality of the human PSP structure

The final model of HPSP (consisting of 412 residues, 390 water molecules, three Ca^{2+} ions and six Cl^- ions) converged to an *R* factor of 21.6% and an R_{free} value of 23.4% (Table 2). There are two molecules in the asymmetric unit, MolA and MolB, with both molecules being almost identical. MolA consists of 205 and MolB of 207 residues out of 225 residues. The superposition of both monomers in the asymmetric unit gives an r.m.s. deviation of 0.67 Å for the C^α atoms (201 residues superimposed). In each molecule of the asymmetric

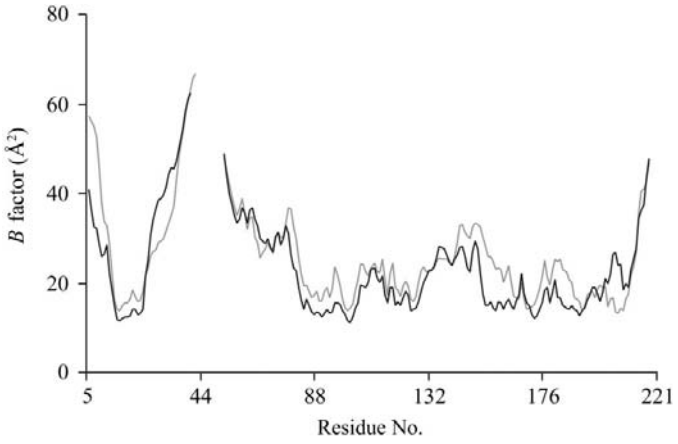

Figure 2
Graphical representation of *B* factors of the main-chain atoms of MolA (thick line) and MolB (thin line) as a function of the residue number. This plot indicates that the missing residues (residues 45–56 for MolA and residues 47–56 for MolB) are located in a region with very high *B* factors.

unit four amino acids at the N-terminus (1–4) and four at the C-terminus (222–225) are disordered. For another 12 amino acids in MolA (45–56) and another ten amino acids in MolB (47–56), there is no visible density in the electron-density maps. As will be discussed later, this unfolded region coincides with the region that discriminates between the open and closed conformation. The *B*-factor plot of the main-chain atoms, shown in Fig. 2, clearly indicates that the missing residues are located in a region of higher than average *B* factors. This is an indication of the mobility of this region in the open conformation of HPSP. The estimated coordinate error of the model is 0.20 Å (Luzzati, 1952). The Ramachandran plot shows that 90.8% of the residues are located in the most favoured regions and 9.2% in the additional allowed regions. No residues are found in the generously allowed regions or in the disallowed regions. The crystallographic *R* factor as a function of the resolution is tabulated in Table 3.

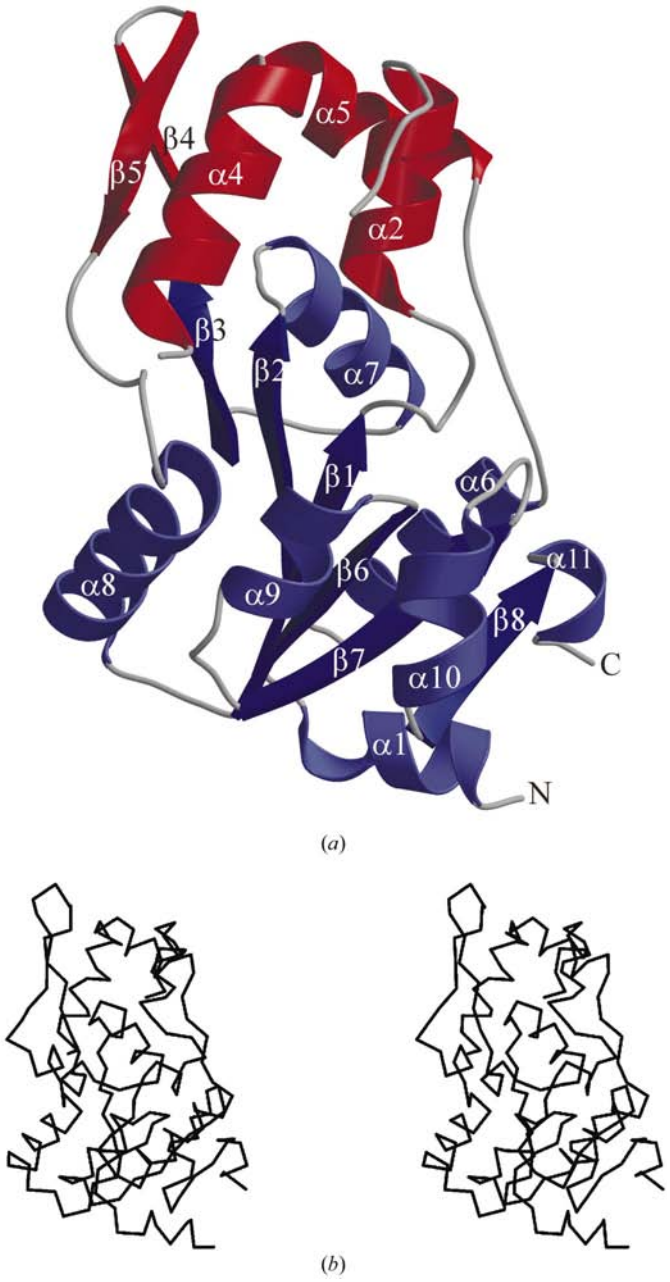

Figure 3
(*a*) Ribbon diagram of the overall three-dimensional structure of one monomer of HPSP in the open conformation. The β-strands are numbered $\beta1$–$\beta8$ and the α-helices $\alpha1$–$\alpha11$. Helix $\alpha3$, connecting helix $\alpha2$ to helix $\alpha4$ in the closed conformation (not shown), is completely disordered in the open conformation and is therefore not visible. The part on top shown in red consists of the helix bundle and the dimer interface $\beta4$ and $\beta5$. The lower part shown in blue is the core domain, which resembles a Rossmann fold. (*b*) Stereoview of the C^{α} trace of one monomer of HPSP.

Table 3
The crystallographic *R* factor as a function of the resolution.

Resolution (Å)	*R*	R_{free}
500.0–3.30	0.1988	0.2135
3.30–2.62	0.2221	0.2279
2.62–2.29	0.2174	0.2218
2.29–2.08	0.2150	0.2413
2.08–1.93	0.2217	0.2644
1.93–1.81	0.2280	0.2496
1.81–1.72	0.2336	0.2571
1.72–1.65	0.2431	0.2634
1.65–1.58	0.2572	0.2723
1.58–1.53	0.2555	0.2756

4.2. Structure description

The ribbon diagram in Fig. 3 shows that one monomer of HPSP consists of two major domains. One domain resembles a Rossmann fold (Rossmann *et al.*, 1974) and the second domain consists of the dimer-interface part and a helix bundle. The core α/β domain, which resembles a Rossmann fold, displays a six-stranded parallel β-sheet ($\beta1$–$\beta3$ and $\beta6$–$\beta8$) surrounded by three α-helices on one side ($\alpha8$–$\alpha10$) and by four α-helices on the other side ($\alpha1$, $\alpha6$, $\alpha7$, $\alpha11$). HPSP is a dimer in solution and the dimer-interface part is located in strands $\beta4$ and $\beta5$. The helix bundle of HPSP in the open conformation consists of three helices ($\alpha2$, $\alpha4$, $\alpha5$) and a missing part for which no electron density can be seen.

Worth mentioning is that the missing part in the helix bundle of HPSP (region 47–56) corresponds to an extra helix of the MJ PSP structure in the closed conformation and to a disordered part (region 40–47) in the open conformation (Wang *et al.*, 2002). A comparison between the HPSP and MJ PSP structures (Fig. 4) clearly shows that this extra helix in MJ PSP covers the active site, preventing the entrance of the substrate.

These findings and the results of a comparison with the HPSP structure in complex with the competitive inhibitor 2-amino-3-phosphonopropionic acid (AP3; Kim *et al.*, 2002) suggest that the present structure has a completely open conformation. Although in the HPSP–AP3 complex one of the two molecules of the dimer is described as being in an open conformation, the helix covering the active site is clearly visible. Therefore, we suggest defining the structure with AP3 as the semi-open state, whereas the structure we present here is the open conformation. HPSP adopts this fully opened state when no substrate or inhibitor is bound to the active site.

4.3. Reaction mechanism of PSP

Structural studies on MJ PSP suggest that the overall PSP reaction, shown in Fig. 5 (Wang *et al.*, 2002), requires a dynamic structure. The reaction mechanism involves nucleophilic attacks with acid/base catalysis. In absence of the substrate L-phosphoserine, PSP is in the open conformation. Binding of the substrate causes a shift to the closed conformation. In this closed conformation, the active site is no longer accessible to the substrate. Asp22 of HPSP serves as the general acid (Enz-H in Fig. 5) donating a proton to serine, the leaving group. In the phosphotransfer step the phosphate group is covalently bound to Asp20. During dephosphorylation, Asp22 acts as the general base (Enz-B in Fig. 5), extracting a proton from the attacking water molecule.

Superposition of the HPSP and the MJ PSP structures shows that the active site of HPSP consists of two parts: one part that binds phosphate and another part that binds serine, as in MJ PSP. The residues that bind phosphate form a cationic cavity. The O atoms of the phosphate group can interact with the side-chain N of Lys158, with the main-chain N of Gly110 and with the Ca^{2+} ion, which would be a Mg^{2+} ion under physiological conditions. In MJ PSP Asn170 is additionally involved in phosphate binding. In HPSP, however, the corresponding residue Thr182 is too far away from the cationic cavity to participate in the binding of phosphate. Nevertheless, one may conclude that the overall binding capacity for phosphate is not affected by this evolutionary mutation.

The serine-binding part of the active site is composed of Glu29 and Arg65, which can form hydrogen bonds with the amino and carboxyl groups of L-phosphoserine, respectively. Since in our HPSP structure no substrate is bound to the active site, the side chain of Glu29 is flexible and no clear density can be seen for this residue. Based on comparison with the previously published MJ PSP complex structure, binding of the substrate would stabilize the side chain of Glu29 in one fixed position towards the amino group of L-phosphoserine. Phe58 and Met43 can form van der Waals contacts with the serine group. Phe58 is in the same position and orientation as the corresponding Phe49 in MJ PSP. Met43 lies in the part that is completely disordered in the open conformation of HPSP. If Met43 is able to form van der Waals contacts with the substrate, the disordered region of the open conformation will be stabilized, inducing the enzyme to switch from the open to the closed conformation. Upon stabilization by these contacts the unfolded region can refold to form a helix, as shown in the closed conformation of MJ PSP in Fig. 4.

Table 4
Distances between the Ca^{2+} ion and the neighbouring atoms in the active site for MolA and MolB.

The typical metal–donor atom target distances for Ca^{2+} and Mg^{2+} are also given (Harding, 2001). This shows that the observed distances in the HPSP structure correspond to typical Ca^{2+} distances.

	Ca^{2+} ion in MolA (Å)	Ca^{2+} ion in MolB (Å)	Target distance (Å) for Ca^{2+} ion	Target distance (Å) for Mg^{2+} ion
Asp20 OD1	2.37	2.23	2.36	2.26
Asp22 O	2.31	2.29	2.36	2.26
Asp179 OD2	2.30	2.33	2.36	2.26
H_2O	2.33	2.30	2.39	2.07
H_2O	2.44	2.49	2.39	2.07
H_2O	2.37	2.41	2.39	2.07

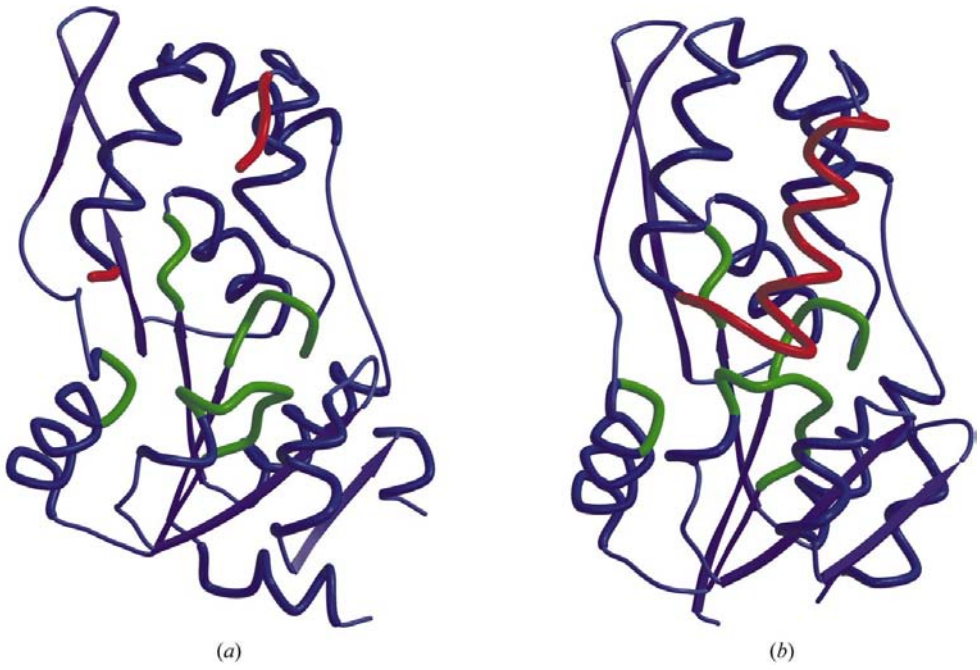

Figure 4
(*a*) HPSP in the open conformation. The helix which can cover the active site is disordered and in this way the active site is easily accessible to L-phosphoserine. Upon binding of the substrate L-phosphoserine, the disordered part is stabilized to form a helix (shown in red) forming the closed conformation (*b*). In this closed conformation the active site is completely shielded and catalysis can occur. After the phosphotransfer has occurred the active site must open again to release the reaction products.

4.4. The effect of Ca^{2+} in the active site

Biochemical studies indicate that Ca^{2+}, unlike Mg^{2+}, does not stimulate phosphoserine phosphatase, but rather inhibits the small activity observed in the absence of added Mg^{2+} (Neuhaus & Byrne, 1959). In the active site of the present structure a Ca^{2+} ion was found instead of an Mg^{2+} ion as in previously reported structures of the PSP family. The presence of the Ca^{2+} ion undoubtedly results from the fact that we used 0.7 *M* $CaCl_2$ in the crystallization conditions and that no Mg^{2+} was present at any point. The presence of a Ca^{2+} ion is further identified by the geometry and the metal–donor atom target distances. All

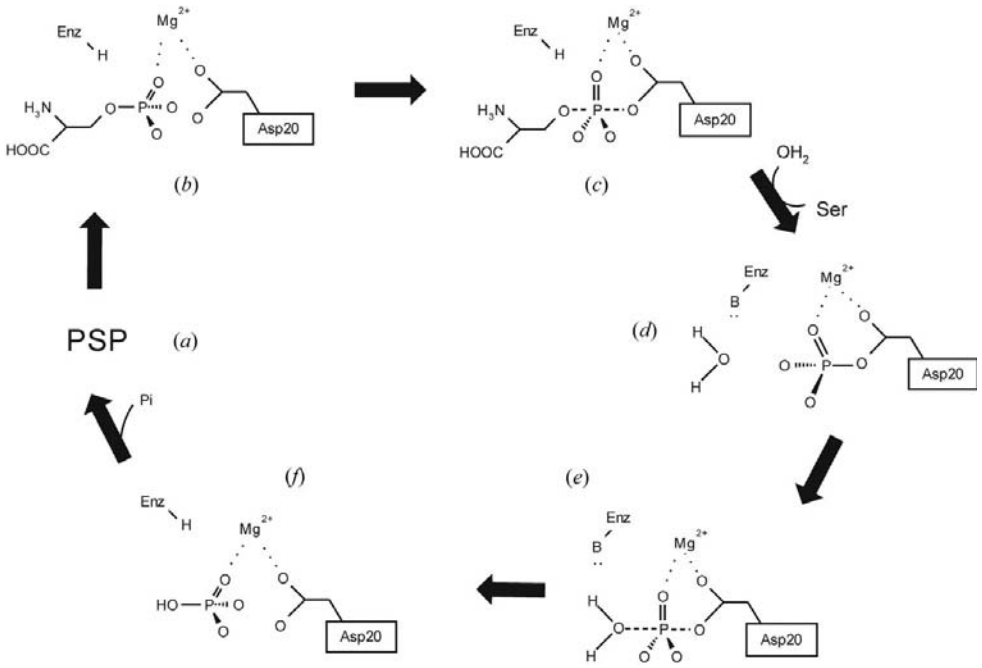

Figure 5
(*a*) General scheme of the reaction cycle of PSP (Wang *et al.*, 2002). (*b*) Open conformation of HPSP. L-Phosphoserine binds to the active site, presenting its phosphate group to Asp20. (*c*) Transition state with nucleophilic attack of Asp20. (*d*) Covalent phospho-aspartyl enzyme intermediate. (*e*) Transition state with a nucleophilic attack of a water molecule causing the dephosphorylation of Asp20. (*f*) Phosphate non-covalently bound in the active site.

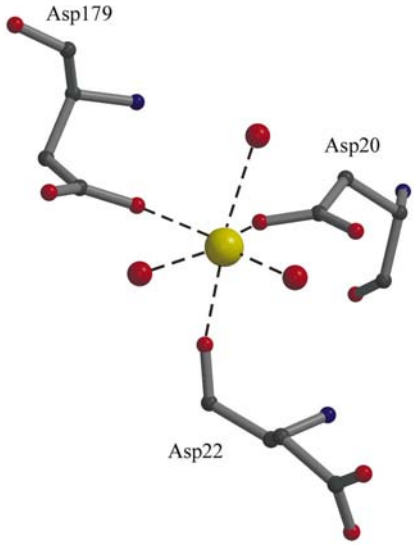

Figure 6
View of the octahedrally coordinated Ca^{2+} ion in the active site. Asp20, Asp22 and Asp179 are represented in ball-and-stick form, with O, C and N atoms coloured red, black and blue, respectively. The Ca^{2+} ion is shown in yellow. Three of the Ca^{2+} ligands are water molecules, shown as red balls, forming hydrogen bonds with the Ca^{2+} ion. The dashed lines represent hydrogen bonds and metal–ligand interactions.

the distances, shown in Table 4, match to a large extent the ideal distances for Ca^{2+}–donor atom combinations (Harding, 2001). Moreover, assessment of the *B* factors indicates that the ion must be a Ca^{2+} ion, because all the surrounding atoms are in the same range of *B*-factor values. Replacing the Ca^{2+} ion by an Mg^{2+} ion causes the *R* factor to increase substantially during the refinement procedure.

The coordination of the Ca^{2+} ion in the active site is octahedral as shown in Fig. 6. Three water molecules and three O atoms (Asp20 OD1, in the main-chain carbonyl group of Asp22 and Asp179 OD2) occupy the six coordination sites of the Ca^{2+}. Asp179 is part of a loop structure that points to the active site for binding of the Ca^{2+} ion. This loop is stabilized by the formation of hydrogen bonds from Asp183 with the main-chain N atoms of Asp179 and Gly180. Just like Asp171 in the MJ PSP, Asp183 is in contact with the active site through a salt bridge with Lys158.

It should be mentioned that substitution of the Mg^{2+} ion by a Ca^{2+} ion in the active site affects the metal–water molecule distances rather drastically (Table 4). This might give an indication of why the same crystallization conditions in which $CaCl_2$ was replaced by $MgCl_2$ yielded no crystals. Since the divalent Ca^{2+} ion is part of the cationic cavity of the active site, it is suggested that Ca^{2+} does not provide the same metal-ligand binding pattern as Mg^{2+} to place L-phosphoserine in the exact orientation for hydrolysis. In MJ PSP the distance between the oxygen O2 of the phosphate part of L-phosphoserine and the Mg^{2+} ion is 2.41 Å (Wang *et al.*, 2002). With a Ca^{2+} ion in the active site this distance would increase and the serine part of L-phosphoserine would no longer be in an ideal position for hydrolysis by the serine-binding part of the active site.

5. Conclusions

The crystal structure described here at a resolution of 1.53 Å provides the first model of HPSP in a completely open conformation. When no substrate or inhibitor is bound to the active site of HPSP, one part of the helix bundle is disordered. In this state the active site is completely open and the entrance of the substrate is in no way hindered. It is probable that the structure in the open conformation as described here is the favourable conformation for L-phosphoserine to enter under physiological conditions.

Evidence is presented that the Mg^{2+} ion in the active site provides the ideal metal-ligand binding pattern for positioning the substrate optimally in the active site. Replacing the Mg^{2+}

ion by a Ca^{2+} ion disturbs the ideal binding network in the active site of PSP and affects the enzymatic activity in a negative way.

AR is a Postdoctoral Research Fellow of the Fund for Scientific Research-Flanders (Belgium), CV is a Postdoctoral Research Fellow of the K.U. Leuven Research Fund and JFC is Chargé de Recherches of the Belgian FNRS. Work in the laboratory of EVS is supported by the Belgian Federal Service for Scientific, Technical and Cultural Affairs and by the FRSM. We thank the beamline scientists at DESY for technical support and the European Union for support of the work at EMBL Hamburg through the Access to Research Infrastructure Action of the improving human potential programme, contact No. HPRI-CT-1999-00017.

References

Abrahams, J. P. & Leslie, A. G. W. (1996). *Acta Cryst.* D**52**, 30–42.
Aravind, L., Galperin, M. Y. & Koonin, E. V. (1998). *Trends Biochem. Sci.* **23**, 127–129.
Brünger, A. T., Adams, P. D., Clore, G. M., DeLano, W. L., Gros, P., Grosse-Kunstleve, R. W., Jiang, J. S., Kuszewski, J., Nilges, M., Pannu, N. S., Read, R. J., Rice, L. M., Simonson, T. & Warren, G. L. (1998). *Acta Cryst.* D**54**, 905–921.
Cho, H., Wang, W., Kim, R., Yokota, H., Damo, S., Kim, S. H., Wemmer, D., Kustu, S. & Yan, D. (2001). *Proc. Natl Acad. Sci. USA*, **98**, 8525–8530.
Collet, J. F., Gerin, I., Rider, M. H., Veiga da Cunha, M. & Van Schaftingen, E. (1997). *FEBS Lett.* **408**, 281–284.
Collet, J. F., Stroobant, V., Pirard, M., Delpierre, G. & Van Schaftingen, E. (1998). *J. Biol. Chem.* **273**, 14107–14112.
Collet, J. F., Stroobant, V. & Van Schaftingen, E. (1999). *J. Biol. Chem.* **274**, 33985–33990.
Dunlop, D. S. & Neidle, A. (1997). *Biochem. Biophys. Res. Commun.* **235**, 26–30.
Furey, W. & Swaminathan, S. (1997). *Methods Enzymol.* **277**, 590–620.
Harding, M. M. (2001). *Acta Cryst.* D**57**, 401–411.
Jaeken, J., Detheux, M., Van Maldergem, L., Frijns, J. P., Alliet, P., Foulon, M., Carchon, H. & Van Schaftingen, E. (1996). *J. Inherit. Metab. Dis.* **19**, 223–226.
Jones, T. A., Zhou, J. Y., Cowtan, S. & Kjeldgaard, M. (1991). *Acta Cryst.* A**47**, 110–119.
Kim, H. Y., Heo, Y. S., Kim, J. H., Park, M. H., Moon, J., Kwan, D., Yoon, J., Shin, D., Jeong, E., Park, S. Y., Lee, T. G., Jeon, Y. H., Ro, S., Cho, J. M. & Hwang, K. Y. (2002). *J. Biol. Chem.* **277**, 46651–46658.
Kraulis, P. J. (1991). *J. Appl. Cryst.* **24**, 946–950.
La Fortelle, E. de & Bricogne, G. (1997). *Methods Enzymol.* **276**, 472–493.
Laskowski, R. A., MacArthur, M. W., Moss, D. S. & Thornton, J. M. (1993). *J. Appl. Cryst.* **26**, 283–291.
Lingrel, J. B. & Kuntzweiler, T. (1994). *J. Biol. Chem.* **269**, 19659–19662.
Luzzati, V. (1952). *Acta Cryst.* **5**, 802–810.
MacLennan, D. H., Clarke, D. M., Loo, T. W. & Skerjanc, I. S. (1992). *Acta Physiol. Scand. Suppl.* **607**, 141–150.
Matthews, B. W. (1974). *J. Mol. Biol.* **82**, 513–526.
Merritt, E. A. & Bacon, D. J. (1997). *Methods Enzymol.* **277**, 505–524.
Neuhaus, F. C. & Byrne, W. L. (1959). *J. Biol. Chem.* **234**, 113–121.
Otwinowski, Z. & Minor, W. (1997). *Methods Enzymol.* **276**, 307–326.
Paudice, P., Gemignani, A. & Raiteri, M. (1998). *Eur. J. Neurosci.* **10**, 2934–2944.
Peeraer, Y., Rabijns, A., Verboven, C., Collet, J. F., Van Schaftingen, E. & De Ranter, C. (2002). *Acta Cryst.* D**58**, 133–134.
Perrakis, A., Morris, R. & Lamzin, V. S. (1999). *Nature Struct. Biol.* **6**, 458–463.
Ridder, I. S. & Dijkstra, B. W. (1999). *Biochem. J.* **339**, 223–226.
Rossmann, M. G., Moras, D. & Olsen, K. W. (1974). *Nature (London)*, **250**, 194–199.
Schell, M. J., Brady, R. O. Jr, Molliver, M. E. & Snyder, S. H. (1997). *J. Neurosci.* **17**, 1604–1615.
Wang, W., Cho, H., Kim, R., Jancarik, J., Yokota, H., Nguyen, H. H., Grigoriev, I. V., Wemmer, D. E. & Kim, S. H. (2002). *J. Mol. Biol.* **319**, 421–431.
Wang, W., Kim, R., Jancarik, J., Yokota, H. & Kim, S. H. (2001). *Structure*, **9**, 65–71.
Wolosker, H., Sheth, K. N., Takahashi, M., Mothet, J. P., Brady, R. O. Jr, Ferris, C. D. & Snyder, S. H. (1999). *Proc. Natl Acad. Sci. USA*, **96**, 721–725.